Proc. of the 8th International Conference NEET 2013, Zakopane, Poland, June 18–21, 2013

Thermal Desorption Studies of Ar^+ Implanted Silicon

A. Drozdziel[a], A. Wojtowicz[a], M. Turek[a,*], K. Pyszniak[a], D. Maczka[b], B. Slowinski[b], Y.V. Yushkevich[c] and J. Zuk[a]

[a]Institute of Physics, Maria Curie-Skłodowska University, Lublin, Poland

[b]National Centre for Nuclear Studies, Świerk-Otwock, Poland

[c]Laboratory of Nuclear Problems, JINR Dubna, Russia

Thermal desorption spectrometry measurements were performed for Ar implanted Si samples. Implantation energy E_{i} varied in the range 85–175 keV. The release of implanted Ar in two steps was observed in the temperature range 930–1300 K: the relatively narrow peak at lower temperature (≈ 930 K for implantation fluence 5×10^{16} cm^{-2}) is due to the release of Ar from the agglomerations (bubbles) while the broader peak observed for higher temperatures (≈ 950 K for implantation fluence 5×10^{16} cm^{-2}) comes from Ar atoms diffusing out of the sample. Inverse order of peaks is observed compared to the results for lower energy implantations (< 50 keV). Analyzing the thermal desorption spectra collected for different heating ramp rates enabled estimation of the desorption activation energy (2 eV for $E_{\mathrm{i}} = 85$ keV and 1.7 eV for $E_{\mathrm{i}} = 115$ keV).

DOI: 10.12693/APhysPolA.125.1400

PACS: 68.43.Vx, 61.72.uf

1. Introduction

Thermal desorption spectroscopy (TDS) of inert gases is a convenient tool enabling studies of the disorder introduced by ion implantation, diffusion, interaction of gases during the desorption and trapping of atoms by vacancies and their clusters [1]. Such technique is successfully used not only in the case of semiconductors widely used in electronic industry [2, 3] but also for implanted metals [4, 5] and thin foils [6]. TDS spectroscopy is also often used to study radiation induced damage and retention of deuterium in plasma facing materials like tungsten [7–9] or beryllium [10].

TDS of inert gases implanted into Si is a suitable technique to find out in what states they are in the host as well as to determine temperatures at which they could be released. TDS spectra of argon implanted silicon samples were obtained for very low (100 eV [11]) and low (1 keV [12]) implantation energies, as well as for moderate energies typical for semiconductor device ion implantation processing (20–60 keV [13]). It was found in [13] that implanted Ar are in two different states in Si, which resulted in two peaks in TDS spectra. The presence of two kinds of peaks was also observed in the case of He implanted SiC [3] and diamond implanted with deuterium [14].

The paper briefly presents the construction of the TDS spectrometer designed and built in Institute of Physics, Maria Curie-Skłodowska University in Lublin. The TDS spectra of Si samples implanted with Ar of energies in the range 85–175 keV are presented and discussed. The desorption activation energy is estimated analyzing spectra measured for different heating ramp rates.

*corresponding author; e-mail: mturek@kft.umcs.lublin.pl

2. Experimental

Schematic view of the thermal desorption spectrometer is shown in Fig. 1. The cylindrical vacuum chamber of inner diameter of 200 mm and height of 200 mm is equipped with 8 flanges enabling connection of mass spectrometer, vacuum meter, dosing valves, electrical feedthroughs, and other equipment. The sample is heated by 50 mm diameter heater (HTR1002 Boralectric, Momentive, Strongsville OH, USA) mounted to the bottom part of the chamber. The heater is shielded by the screens made of 0.5 mm thick Mo plates, as well as by thicker, 2 mm stainless steel plate (bottom shield). The heater is powered by a programmable power supply EA-PS 8000T (EA Electro-Automatik GmbH, Viersen, Germany), enabling the heating with different profiles and heating rates up to 1600 K. Sample temperature is measured using the K-type thermocouple connected via Hewlett–Packard 34970A data acquisition/switch unit to the PC-class computer that controls the whole system. The alternative temperature measurement is possible using a pyrometer (CT2M, Optris GmbH, Berlin, Germany). The pyrometer head is mounted above the quartz glass window in the central part of the upper cover and gives possibility of contactless measurements of the sample surface, which is especially important in the case of temperature ranges higher than working range of K-type thermocouple.

The base pressure of 1×10^{-7} mbar is provided by the turbomolecular vacuum pump (Balzers TPM 260) with a rotary vane forevacuum pump. Pressure measurements are done by TPG 261 vacuum meter (Pfeiffer Vacuum, Asslar, Germany) with the cold cathode gauge.

Gases released from the heated specimen are registered by the QMG220 quadruple mass spectrometer (Pfeiffer Vacuum, Asslar, Germany) controlled by the Quadera™ software.

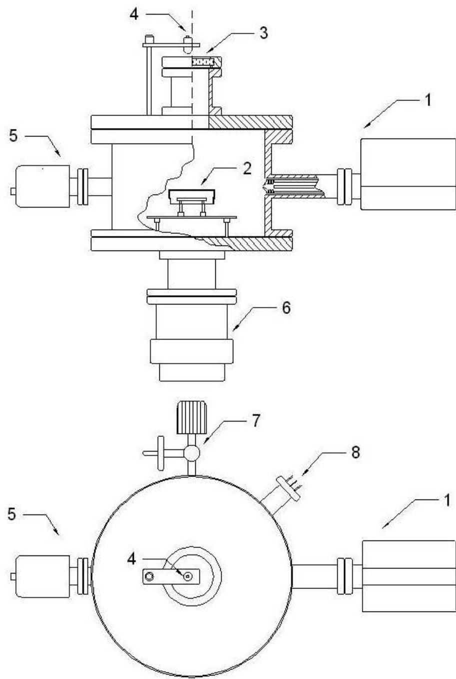

Fig. 1. Schematical drawing of the TDS spectrometer: 1 — quadruple mass spectrometer, 2 — shielded heater, 3 — quartz glass window, 4 — pyrometer head, 6 — turbomolecular pump, 7 — dosing valve, 8 — electric feedthrough.

The boron doped 100-oriented silicon wafers were implanted with Ar^+ ions incident normally to the sample surface using the ion implanter in the Institute of Physics, Lublin, equipped with the versatile arc discharge ion source [15–19]. Implantation energies varied in the range 85–175 keV. The fluence was 5×10^{16} ions/cm^2, while the beam current density was approximately 1 μA/cm^2.

The TDS heater was annealed before measurements in order to get rid of most of residual gases. The spectra were collected during the sample heating with the linear ramp

$$T(t) = T_0 + \beta t, \quad (1)$$

where T_0 is the initial (room) temperature and β is the ramp rate. The specimens (of the size of ≈ 2 cm^2) were heated with the ramp rate of 0.1 K/s and 0.3 K/s. The signal corresponding to the 40 a.m.u. (Ar) was registered by the mass spectrometer. As the TDS spectrometer chamber was pumped down during the measurement the registered signal corresponds to the Ar release rate.

3. Results and discussion

Figure 2 presents the most important parts of the TDS spectra collected in the case $\beta = 0.1$ K/s. The release of residual gases was observed as a broad peak in the range 300–600 K. The narrow peak (A) is observed for temperatures 930–940 K. It corresponds to the Ar release from agglomerates (bubbles) that are known to be formed during high-fluence inert gases implantations. Let us note that the rapid release consists usually of several (2–4) phases, especially well-visible for lower implantation energies (85 and 115 keV). The existence and random structure of these sub-peaks may suggest that one may deal with a kind of percolation or rapid ruptures of the bubbles resulting from the build-up of the gas pressure [20, 21].

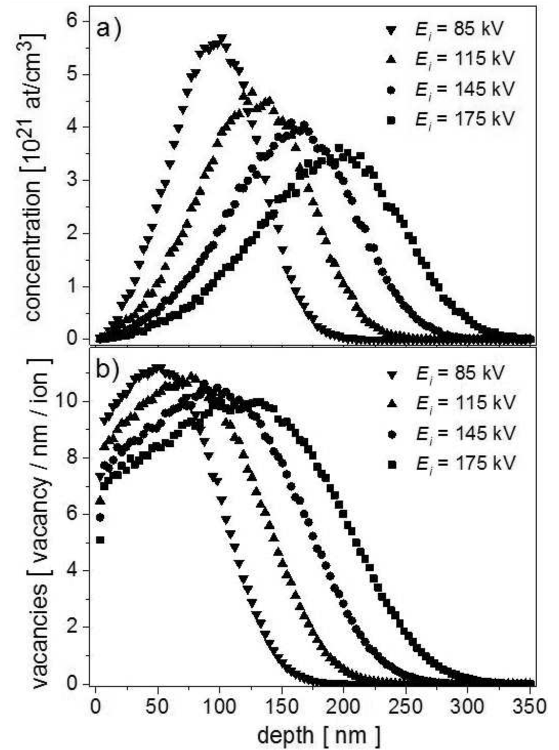

Fig. 2. Implanted Ar concentration (a) and damage (vacancies) distributions (b) calculated using the SRIM code.

The second type of Ar release, being a diffusion controlled process, is observed for slightly higher temperatures ($\approx$ 950–960 K) as a broad peak. It should be mentioned here that such two-peak structure of TDS spectra was discussed in [13]. Let us note that for lower implantation energies (20–60 keV) the different order of the observed peaks: the diffusion driven peak was observed earlier, as the projected ranges of implantations were much smaller. The authors of paper [13] stated also that the peak A disappears for E_{i} larger than 50 keV, while in the light of the inverse order observed for $E_{\mathrm{i}} = 85$ keV and higher one should rather conclude that peaks A and B simply overlap. The shape of the B peak changes with increasing E_{i}: for smaller E_{i} it is narrower and well--defined while for 145 keV and 175 it becomes flat and much smaller than the peak A.

The described effect may be the result of the differences between the projected implantation ranges R_{p} (the highest Ar concentration) and the depth of maximal radiation damage R_{D}, where cavities are formed. Figure 3 presents Ar concentration and Frenkel pair distributions

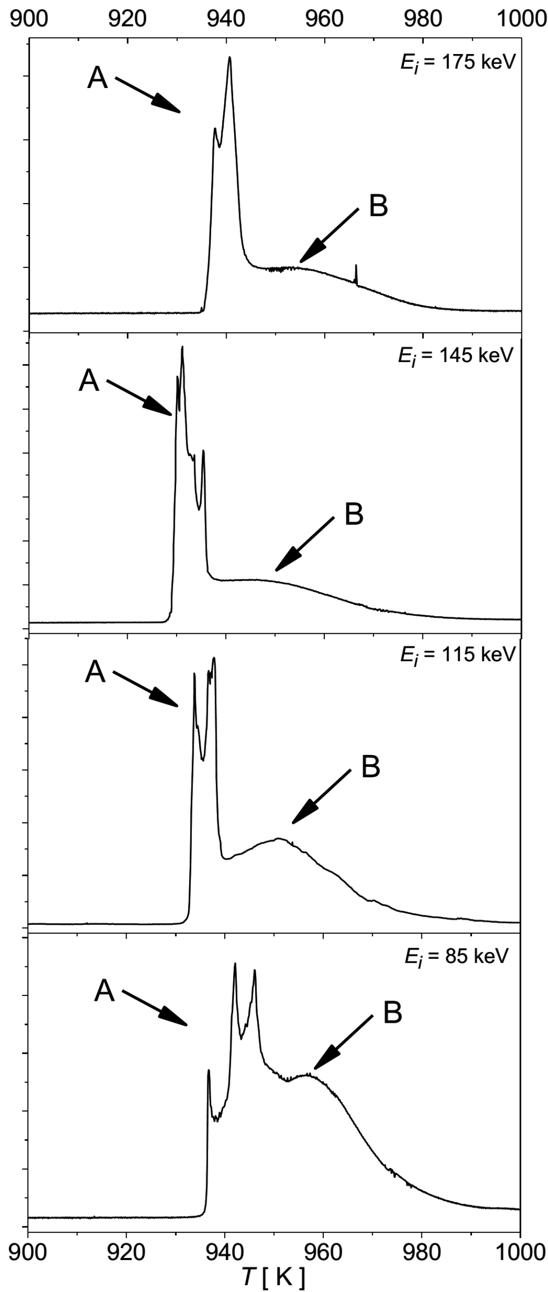

Fig. 3. TDS spectra of Ar implanted into Si collected for $\beta = 0.1$ K/s.

obtained using the SRIM code [22]. It should be noted that in the case of $E_{\rm i} = 85$ keV $R_{\rm p}$ is 85 nm while $R_{\rm D}$ is approximately 50 nm, and the initial Ar concentration at the depth $R_{\rm D}$ is below 35% of that at $R_{\rm p}$ (the Ar distribution is narrower and closer to the surface and the zone of cavity formation). On the other hand, the Ar concentration at $R_{\rm D}$ (≈ 140 nm) for $E_{\rm i} = 175$ keV reaches 70% of that at $R_{\rm p}$ and the Ar distribution profile is much wider. Assuming that the B peak comes (at least partly) from the diffusing Ar atoms that reached cavities and then immediately the surface (due to the ruptures), the flattening of B peaks is the result of the flattening of concentration profiles shown in Fig. 3a. The inverse order of peaks for $E_{\rm i}$ may be the result of much smaller $R_{\rm p}$ for lower energy implantation and, consequently, shorter time the diffusing Ar atoms need to reach the sample surface, compared to the bubble pressure build-up time.

TABLE

Parameters enabling estimation of the desorption activation energy according to the Redhead method.

$E_{\rm i} = 85$ keV			$E_{\rm i} = 115$ keV		
β [K/s]	$T_{\rm p}$ [K]	Q [eV]	β [K/s]	$T_{\rm p}$ [K]	Q [eV]
0.1	956	2.0	0.1	951	1.7
0.3	997		0.3	998	

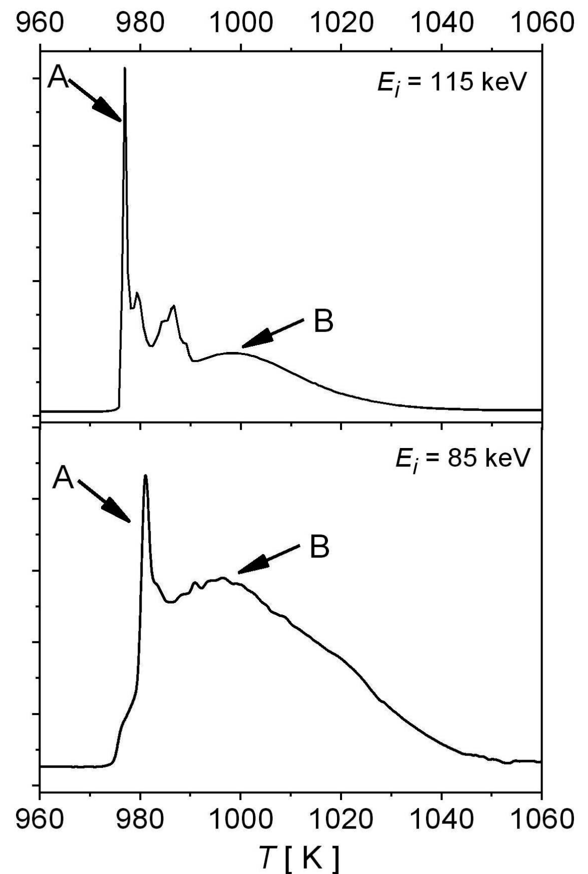

Fig. 4. TDS spectra of Ar implanted into Si collected for $\beta = 0.3$ K/s.

The TDS spectra were also collected for $\beta = 0.1$ K/s. Examples for $E_{\rm i} = 85$ and $E_{\rm i} = 115$ are shown in Fig. 4. As one can see, both peaks appear at temperatures higher than previously (peaks A at $\approx$ 975–980 K and B at $\approx$ 995–1000 K). This B peak shift enables estimation of desorption activation energy using the Redhead approach [23]. The first order desorption is described by the equation

$$r(t) = \frac{\mathrm{d}n}{\mathrm{d}t} = -\gamma n \exp\left(-\frac{Q}{kT}\right), \qquad (2)$$

where n is the surface density of the desorbing substance, $r(t)$ is the desorption signal, k is the Boltzmann constant, Q is the desorption activation energy and γ is the pre--exponential factor. Assuming the linear heating ramp and denoting the temperature corresponding to the maximum of the B peak as T_{p}, one obtains from the condition $\mathrm{d}r/\mathrm{d}t = 0$ the relationship

$$\frac{1}{T_{\mathrm{p}}} = \frac{k}{Q}\ln\left(\frac{T_{\mathrm{p}}^2}{\beta}\right) + \frac{k}{Q}\ln\left(\gamma\frac{k}{Q}\right). \qquad (3)$$

Hence, the diffusion activation energy could be easily obtained from the $1/T_{\mathrm{p}}$ vs. $\ln(T_{\mathrm{p}}^2/\beta)$. Values of T_{p} and the results of Q estimations are gathered in Table.

4. Summary

The brief description of the setup enabling thermal description spectroscopy studies built recently in Institute of Physics (MCSU Lublin) is given in the paper. The TDS spectra of argon were measured for Ar implanted (85–175 keV) silicon samples. Two kinds of peaks were observed, as in the case of lower implantation energies ($<$ 50 keV), which confirms that implanted Ar ions are in two states. It was shown that the peak corresponding to the Ar release from bubbles is present also for $E_{\mathrm{i}} > 50$ keV, despite the conclusions in [13]. The order of peaks is inversed, compared to that presented in [13]. The spectra were collected for two heating ramp rates, which enabled estimation of diffusion activation energy according to Redhead method ($Q = 2.0$ eV for $E_{\mathrm{i}} = 85$ keV and $Q = 1.75$ eV for $E_{\mathrm{i}} = 115$ keV).

Changes of TDS spectra with the Ar implantation fluence will be subject of further studies. Extension of investigations to other popular dopants like Al, N, In, As is also planned.

References

[1] A.A. van Gorkum, E.V. Kornelsen, *Vacuum* **31**, 89 (1981).

[2] G.F. Cerofolini, G. Calzolari, F. Corni, S. Frabboni, C. Nobili, G. Ottaviani, R. Tonini, *Phys. Rev. B* **61**, 10183 (2000).

[3] E. Oliviero, M.F. Beaufort, J.F. Barbot, A. van Veen, A.V. Fedorov, *J. Appl. Phys.* **93**, 231 (2003).

[4] D. Edwards, *J. Appl. Phys.* **46**, 1444 (1975).

[5] R. Hanada, S. Haito, *CYRIC Reports* **1994**, 13 (1994).

[6] V.A. Belous, A.S. Kuprin, N.S. Lomino, V.D Ovcharenko, E.N. Reshetnyak, O.M. Morozov, V.I. Zhurba, G.N. Tolmachova, *Proc. NAP* **1**, 04RES07 (2012).

[7] M.H.J. 't Hoen, B. Tyburska-Püschel, K. Ertl, M. Mayer, J. Rapp, A.W. Kleyn, P.A. Zeijlmans van Emmichoven, *Nucl. Fusion* **52**, 023008 (2012).

[8] V. Kh. Alimov, B. Tyburska-Püschel, S. Lindig, Y. Hatano, M. Balden, J. Roth, K. Isobe, M. Matsuyama, T. Yamanishi, *J. Nucl. Mater.* **420**, 519 (2012).

[9] R. Kurata, M. Kobayashi, S. Suzuki, W. Wang, N. Ashikawa, A. Sagara, N. Yoshida, Y. Oya, K. Okuno, *J. Plasma Fusion Res.* **9**, 193 (2010).

[10] Y.M. Zakaria, *Thermal Desorption Analysis of Helium Trapping in Ion-Implanted Beryllium*, Open Access Dissertations and Theses, Paper 2371 (1996).

[11] W.M. Lau, I. Bello, L.J. Huang, X. Feng, M. Vos, I.V. Mitchell, *J. Appl. Phys.* **74**, 7105 (1993).

[12] A. Filius, A. van Veen, K.R. Bijkerk, J.H. Evans, *Radiat. Eff.* **108**, 1 (1989).

[13] R. Hanada, S. Saito, S. Nagata, S. Yamaguchi, T. Shinozuka, I. Fujioka, *Mater. Sci. Forum* **196-201**, 1375 (1995).

[14] H. Kimura, M. Sasaki, Y. Morimoto, T. Takeda, H. Kodama, A. Yoshikawa, M. Oyaidzu, K. Takahashi, K. Sakamoto, T. Imai, K. Okuno, *J. Nucl. Mater.* **337-339**, 614 (2005).

[15] M. Turek, S. Prucnal, A. Droździel, K. Pyszniak, *Nucl. Instrum. Methods Phys. Res. B* **269**, 700 (2011).

[16] M. Turek, A. Droździel, K. Pyszniak, S. Prucnal, D. Mączka, Yu. Yushkevich, Yu.A. Vaganov, *Instrum. Exp. Tech.* **55**, 469 (2012).

[17] M. Turek, A. Droździel, K. Pyszniak, S. Prucnal, *Nucl. Instrum. Methods Phys. Res. A* **654**, 57 (2011).

[18] M. Turek, S. Prucnal, A. Droździel, K. Pyszniak, *Rev. Sci. Instrum.* **80**, 043304 (2009).

[19] M. Turek, A. Drozdziel, K. Pyszniak, S. Prucnal, J. Żuk, *Przegląd Elektrotechniczny* **7**, 193 (2010) (in Polish).

[20] K. Wittmaack, P. Blank, W. Wach, *Radiat. Effects* **39**, 81 (1978).

[21] S.K. Erents, G.M. McCraken, *Radiat. Effects* **18**, 191 (1973).

[22] J.F. Ziegler, M.D. Ziegler, J.P. Biersack, *Nucl. Instrum. Methods Phys. Res. B* **268**, 1818 (2010).

[23] P.A. Redhead, *Vacuum* **12**, 203 (1962).